Universitat Autònoma de Barcelona

A Thesis for the

Master in Telecommunication Engineering

Simulation of WLAN Based V2X Signal Models Using Deterministic Channel

by

Mohamed Yousif Norelhuda Elhag

Supervisors

Eloi Ramon Garcia

Departament d'Enginyeria Electrònica
Escola Tècnica Superior d'Enginyeria (ETSE)
Universitat Autònoma de Barcelona (UAB)

Muhanad Mustafa Humaida

Network Department
Canar Telecommunication CO.LT

September 2020

UAB

El sotasignant, Eloi Ramon i Garcia, Professor de l'Escola Tècnica Superior d'Enginyeria (ETSE) de la Universitat Autònoma de Barcelona (UAB),

CERTIFICA:

Que el projecte presentat en aquesta memòria de Treball Final de Master ha estat realitzat sota la seva direcció per l'alumne Mohamed Yousif Norelhuda Elhag.

I, perquè consti a tots els efectes, signa el present certificat.

Bellaterra, 26 de setembre de 2020.

Signatura: Eloi Ramon i Garcia

Resum:

La comunicació Vehicle to Everything (V2X) és un dels temes importants en el camp de les telecomunicacions que pretén proporcionar una gran millora en el sector del transport augmentant la seguretat i el confort durant la conducció, així com reduint la congestió i els accidents de trànsit i, per tant, hi ha d'investigacions, desenvolupaments i inversions realitzades en aquest camp.
Aquesta tesi presenta l'ús del programa de motors de jocs Unity 3D per a la creació d'un model de canal determinista a través del qual podem analitzar i estudiar el rendiment dels models de senyal basats en WLAN que s'utilitzen al Vehicle to everything (V2X). El simulador V2X es va utilitzar per al procés de creació de canals i avaluació del rendiment fent ús de les seves mesures estocàstiques en temps real.
Es van utilitzar dos mètodes diferents per avaluar el rendiment dels models de senyal IEEE 802.11p i 802.11bd amb càlculs diferents, però finalment aquest últim va resultar ser millor, ja que es considera la versió més avançada i última de la família IEEE 802.11

Resumen:

Vehicule to Everything (V2X) es uno de los temas importantes en el campo de las telecomunicaciones con el objetivo de proporcionar una gran mejora en el sector del transporte al aumentar la seguridad y la comodidad durante la conducción, así como reducir la congestión del tráfico y los accidentes y, como resultado, hay muchos de las investigaciones, desarrollos e inversiones realizadas en este campo.
Esta tesis presenta el uso del programa de motor de juegos Unity 3D para la creación de un modelo de canal determinista a través del cual podemos analizar y estudiar el desempeño de los modelos de señal basados en WLAN que se utilizan en la tecnología Vehicule to everything (V2X). El simulador V2X se utilizó para el proceso de creación de canales y evaluación de desempeño haciendo uso de sus medidas estocásticas en tiempo real.
Se utilizaron dos métodos diferentes para evaluar el rendimiento de los modelos de señal IEEE 802.11py 802.11bd con diferentes cálculos, pero finalmente el último resultó ser el superior, ya que se considera la versión más avanzada y más reciente de la familia IEEE

Summary:
Vehicle to everything (V2X) communication is one of the important topics in the telecommunication field aiming to provide a great improvement in the transport sector by increasing safety and comfort while driving as well as reducing traffic congestion and as a result there are a lot of researches , developments and investments made in this field.
This thesis presents the use of Unity 3D game engine program for the creation of a deterministic channel model through which we can analyse and study the performance of the WLAN based signal models that are used in the vehicle to everything (V2X) technology.AN open source V2X simulator was used for the process of channel creation and performance assessment making use of its real time stochastic measurements .
Two different methods were used to assess the performance of both the IEEE 802.11p and 802.11bd signal models with different calculations but eventually the latter proved to be the superior since it is considered the most advanced and latest version of the IEEE 802.11 family.

Table of Contents

List of Figures

List of Tables

Acknowledgment

This project was completely developed in the Network Department at Canar Telecommunication Company in Sudan under the Supervisions of Mr.Muhanad Mustafa Humaida to whom I express my gratitude and appreciation for the endless support and guidance throughout the project .I would also like to thank my supervisor from the Autonomous University of Barcelona DR. Eloi Ramon Garcia for his indispensable remotely supervision and instructions through the writing process of the thesis.
I would like to thank all the professors whom I was honoured to be taught by them at the Autonomous University of Barcelona and a special thanks to the coordinator of the Telecommunication master program Mr. Gary Junkin for his continues advices and solutions for the different difficulties throughout the Master Program

List of Abbreviations

3GP	3rd Generation Partnership Project
16-QAM	16-Quadrature Amplitude Modulation
64-QAM	64- Quadrature Amplitude Modulations.
AWGN	Additive white Gaussian Noise
BCC	Binary Convolution Coding
BPSK	Binary phase shift keying
CSMA	Carrier Sense Multiple Access
C-V2X	Cellular V2X
CIR	Channel Impulse Response
CCA	Clear Channel Assessment
CVS	Comma Separated Values
CW	Contention Window
CP	Cyclic Prefix
DCM	Data Communication module
DSRC	Dedicated Short Range Communication
EPS	Evolved Packet Switching
FSLF	Free Space Loss Factor
IFFT	Inverse Fast Fourier Transform
IEEE	Institute of Electrical and Electronics Engineers
LOS	Line of sight
LDPC	Low density parity check
BLER	Block Error Rate
MAC	Media Access Control
MIMO	Multiple input multiple output
MPC	Multipath Components
MCS	Modulation and Coding Schemes
NGV	Next Generation V2X
NLOS	Non line of sight
OFDM	Orthogonal Frequency Division Multiplexing
PER	Packet Error Rate
PDF	Probability Density Function
PHY	Physical
PLCP	Physical Layer Convergence Protocol
QPSK	Quadrature phase shift keying
RSU	Remote Switching Unit
RX	Receiver
STBC	Space Time Block Coding
TGbd	Task Group 802.11bd
TX	Transmitter
UE	User Equipment
V2X	Vehicle to Everything
V2V	Vehicle to Vehicle
V2I	Vehicle to Infrastructure
V2P	Vehicle to Pedestrian
V2N	Vehicle to Network
WAVE	Wireless Access in Vehicular Environment
WLAN	Wireless Local Area NetworK

Chapter 1

Introduction

At this modern age, vehicles play a great role in our daily life as well as the transport sector however, the increase in population followed by the rapid development in the manufacture and management of the automobile industry escalated the number of vehicles in streets which resulted in a significant increase in the number of car accidents and traffic congestions that are considered a major drawback in the transport sector. Here comes the role of the V2X technology where it acts as a cross-industry event combining both the communication and automotive fields utilizing their latest generation of information and technology so as not to only solve the previously mentioned issues, but has much significance for improving transport efficiency and infrastructure and other inventive solutions and services.[1]

1.1 Background

Vehicle to everything is a term that describes a vehicular communication system with the ability of sending and receiving information to and from any other entity that affects the vehicle. It is formed by combining other communication technology types depending on the participants with which the vehicle exchange data such as the vehicle-to-vehicle (V2V), vehicle-to-Infrastructure (V2I), vehicle-to-pedestrian (V2P), and vehicle-to-network (V2N).A V2X system can be based on one of the two data transfer technologies which are the Cellular based and the Wireless Local Area Network (WLAN) based where the latter is what we focused on in this thesis.

In 2012 the first WLAN based V2X was introduced by the Institute of Electrical and Electronics Engineers (IEEE) that uses the Dedicated Short Range Communication (DSRC) technology which support the transfer of data between vehicles (V2V) and between vehicle and infrastructure (V2I).This radio communication technology is also referred to as IEEE 802.11P. Toyota company was the first to introduce automobiles that use the DSRC technology in 2016.[1]

In 2016 The 3rd Generation Partnership Project (3GPP) introduced the first cellular based V2X system (C-V2X) that support (V2V),(V2I) and also (V2N).Over the years, Studies and

researches made on both as IEEE 802.11P and C-V2X showed that both technologies failed to serve the communication system of high reliability to match the critical and safety applications of the next generation automobiles that are being developed every day[2] .In 2019 the IEEE Task Group 802.11bd (TGbd) was formed as a modification of the 802.11P and aiming to increase the V2X performance and reliability and to support more mode of operations and applications. This state of art is also referred to as the next generation V2X (NGV) i.e. IEEE802.11bd.[2]

1.2 Objective and Aim

A lot of researches and studies are made in the V2X technology most of them focusing in the comparison between WLAN based and cellular based signal model performance, however, this thesis is more about performing different and simpler approaches so as to conduct tests and measurements through which we can assess the salient features and key mechanisms of the signal models. Two approaches where made in order to achieve the required objective which are the deterministic approach in which we created our own channel model and scenario using Unity 3D game program that depend on ray tracing to get a better description of the channel where both the IEEE 802.11p and IEEE 802.11bd are analyzed .The second approach is the use of already programmed stochastic real time measurements and scenarios for the channel model found in a V2X simulator suggested by Canar Company that is also used for measuring the performance of the signal models in terms of throughput and Packet Error Rate (PER).

The process of the deterministic channel creation was the most difficult procedure in this project since it was done using the Unity 3D game engine that requires the understanding of its functions and methodology so as to be able to use it. Also the V2X simulator needed studying due to the fact that it contains a lot of coded functions and formulas each with an important role in our project.

1.3 Thesis outline

Chapter Two: provides theoretical information about the V2X technology and its applications as well as the signal models and the channel properties and models that affect our signal.

Chapter Three: describes the methods and procedures used so as to analyze the WLAN based signal models .

Chapter Four: presents the results of the various simulations and calculations carried out through the project and their analysis .

Chapter Five: Provides a general conclusion of the thesis and presents ideas that might be included in future work

Chapter 2

Theory

This chapter provides a detailed information of the V2X technology including its mode of operation and applications .It also highlight the IEEE Signal models and the channel models that are used in this thesis and their properties.

2.1 V2X Technology

V2X is a series of computing and communicating devices (nodes) sharing data through high-bandwidth, low-inactivity and high-reliability links so as to ensure an efficient traffic flow, improving vehicular safety and optimizing traffic congestion and accidents. After the implementation of V2X, the number of road deaths has been reduced in the EU by 57.5% between 2001 and 2017.[3] Most of the accidents occur in roads and urban areas due to poor visibility, difficult to see obstacles, and mixed traffic . Hence V2X is a reliable non-line of sight (NLOS) system that works in all the environments and even in worst weather conditions by alerting the drivers in form of warnings that appear inside the vehicle thus reducing accidents and improving road safety in the modern-day environment. Depending in the elements associated in the communication , V2X technology is divided into :

- **Vehicle-to-Vehicle (V2V):** vehicles share data among each other to make better decisions . Data exchanged can be vehicle information , traffic status, location, and perception information. In case of a limited range V2V communication, if the direct communication range of V2V is limited, the data can be forwarded by infrastructure based V2V communications that act as transceivers such as Remote Switching Unit (RSU).
- **Vehicle-to-Infrastructure (V2I):** Data is exchanged between vehicles and Remote Switching Unit (RSU) that receive the broadcast message and transmits the message to one or more user equipment (UEs) that supporting V2I application. Information exchanged can be available parking space, traffic congestion and road condition.
- **Vehicle-to-Pedestrian (V2P):** Data is exchanged between vehicles and pedestrians who send and receive messages via their phones or other wireless devices. The

communication is done even when they are in Non-Line of Sight (NLOS) and under different weather conditions.

- **Vehicle-to-Network (V2N):** Data is exchanged between vehicles and servers that provide V2N applications through Evolved Packet Switching (EPS)

2.1.1 V2X Applications:

- **Safety Application**: where the drivers and the pedestrians are frequently updated about the road conditions so as to help them in making early countermeasures to prevent severe catastrophes and accidents. Such information can be like Forward collision warning, Control loss warning, Wrong way driving warning and Pre-Crash sensing warning.
- **Environmental Applications** : where drivers are notified to be driving at a certain speed that reduces the fuel consumption and hence reducing emission of carbon dioxide gas. Also by supplying the driver with updated maps and traffic status to avoid congestion thus reducing high carbon dioxide exposure.
- **Non safety Applications:** applications that increase the comfort for drivers like reducing travel time and improving traffic efficiency by controlling the navigation vehicles and supply drivers with important information on parking congestion and rates. They also include application that provide for drivers and their passengers infotainment content delivery, Web access, and audio and video streaming.[4]

2.1.2 V2X Data Sharing Technologies:

There are currently two underlying technologies that a V2X communication system can be based on which are the WLAN based that uses dedicated short-range communications (DSRC) technology and cellular based vehicle-to-everything (C-V2X) communication technologies. Both technologies have their similarities as well as differences since they were parallel developed by IEEE (DSRC) and 3GGP (C-V2X). DSRC depends on the IEEE 802.11p standard and is used for V2V, V2I and V2P data transfer between vehicles, inter-roadside infrastructure and pedestrians when its distance is limited to a few hundred meters. However, DSRC has been challenged by lack of scalability and lack of performance in highly mobile scenarios. The C-V2X connection allows for increased coverage of streams of data

transmitted and each cellular station broadcasts information to all devices within its coverage through a unicast[5]. But as the vehicles increase the number of unicast streams increase , thereby straining network resources that results in greater messaging latency .Still due to its additional link budget, better congestion control, reliability, interference and better non line of sight capabilities C-V2X offers superior performances to DSRC.[6]

2.2 Signal models

The IEEE standards drive the functionality capability and interoperability of a range of products and services in the Telecommunication field that affect the way people live, work and commute.[7] An example of this products are the signal models which are used in the WLAN based V2X communications .By signal models we means the technologies and means by which signals and data are sent between entities forming the V2X system. There are two types of WLAN based signal models used in the V2X systems , One is the IEEE 802.11p model and the other is the next generation model which is called IEEE 802.11bd which is the most developed and up-to-date

2.2.1 IEEE 802.11p

The 802.11p Task Group was formed in November 2004 but drafts were developed from 2005 through 2009. By 2012, the IEEE 802.11p V2X standard was introduced for wireless local area networks which uses the same modulation and coding schemes as IEEE 802.11a[4]. It was designed from the beginning to meet every V2X application requirement with the most stringent performance specifications and has many favorable features that make it appropriate for road safety and traffic efficiency applications it uses Dedicated short range communications that exchange information among neighboring vehicles at a very small delay compared to an indirect transmission via an infrastructure hence network management is reduced to an absolute minimum without the help of a basic service set (BSS), which is required in 802.11 standards [4]. IEEE 802P features :

- It supports data rates ranging from 3 to 27 Mbps
- coding rates used are 1/2, 2/3 or 3/4 convolutional coding and BPSK (binary phase shift keying), QPSK (quadrature phase shift keying), 16-QAM (16-quadrature amplitude modulation) or 64-QAM modulations.

- Channel bandwidth can be 10 MHz with subcarrier spacing of 0.15 MHz which contain 64 sub-carriers from which 52 are used for data transmission which are also further composed of 48 sub-carriers with 4 pilot sub-carriers as shown in 2.1 [4].
- Support Physical Layer Convergence Protocol (PLCP) that form an Orthogonal Frequency Division Multiplexing frame by shifting the Packet Data Unit coming from the Media Access Control (MAC) layer.
- Depend on the Binary Convolution coding (BCC) technique for error correcting.

Parameters	
Bit rate (Mb/s)	3, 4, 5, 6, 9, 12, 18, 24, 27
Modulation mode	BPSK,QPSK,16QAM,64QAM
Number of sub-carriers	52
Subcarrier spacing	0.15625 MHz
Code rate	1/2, 2/3, 3/4
Guard time	1.6 µs
FFT period	6.4 µs

Table 2.1: PHYs implementation in IEEE 802.11p

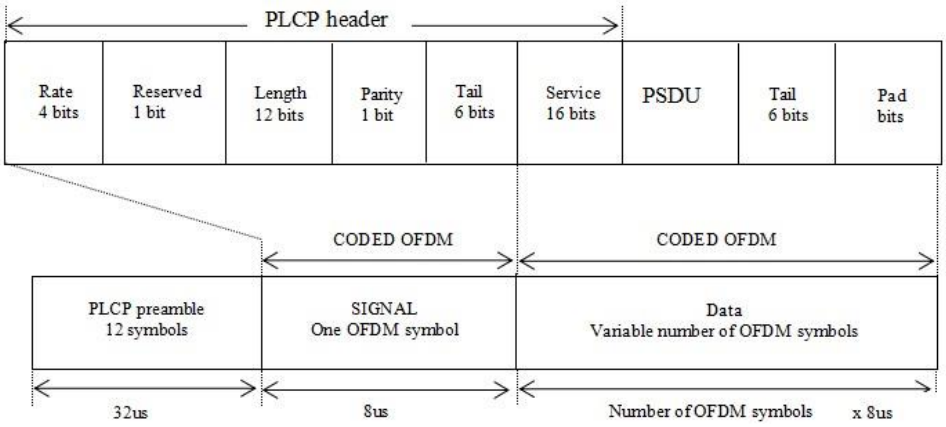

Figure 2.1: Frame format of IEEE 802.11p

2.2.1.1 Dedicated Short Range Communications (DSRC)

Also known as wireless access in vehicular environment (WAVE) and is basically defined from PHY and MAC layers of IEEE 802.11p standard, which is largely derived from IEEE 802.11a standard [8] . The range of this dedicated channel is 5.825 to 5.925 GHz and depend on half clock Orthogonal Frequency Division Multiplexing (OFDM) as a PHY layer which

reduces the 20 MHz spectrum to 10 MHz doubles the OFDM symbol duration with the cyclic prefix. This compensates the Doppler spread due to the high speed of vehicles and make the signal more robust against fading.

Carrier Sense Multiple Access (CSMA) is one of the MAC protocols used in DSRC [6]. In CSMA, a node has to sense the radio channel before transmitting a packet. The node will not transmit if another node is using the channel. If the channel is sensed as idle, the node can start its transmission. If the channel is sensed as busy, the node defers its transmission until the end of the current transmission. The radio channel is sensed as busy when the vehicle detects a signal with a received power strength higher than the Clear Channel Assessment (CCA) threshold. The CCA threshold must be higher than the receiver's sensitivity level (or sensing power threshold). At the end of the channel busy period, the node waits for a backoff time to minimize collisions during contention between multiple nodes that also deferred their transmission. This time is calculated for each packet by multiplying the parameter a Slot Time and an integer number that is randomly selected in the interval [0,CW]; CW is referred to as the Contention Window.[7] The standard sets CW = aCWmin = 15 and a Slot Time =13μs for transmitting broadcast packets in 10 MHz channels. The node decreases the backoff time when it senses idle the channel. The node can start its transmission when its backoff time reaches zero.

DSRC scalability and performance degrades if the vehicle density increases, which is due to two main factors, i.e., packet collisions from simultaneous transmissions and the hidden node problem. To overcome these issues, IEEE 802.11 and the 3GPP are focusing on next-generation V2X systems and have created a task force called IEEE 802.11 next-generation V2X (NGV)[9]. A new and updated IEEE 802.11bd was introduced for V2X communications. IEEE 802.11bd is an advanced form of existing 802.11p by leveraging the MAC and PHY options of 802.11n/ac/ax [7]. It overcomes the issues related to 802.11p in terms of MAC throughput, interoperability and Doppler shift.

2.2.2 IEEE 802.11bd

To overcome the issues, related to IEEE 802.11p, A new and updated IEEE 802.11bd was introduced for V2X communications that showed enhancements in terms of MAC throughput, interoperability, Doppler shift .The main specifications and features of IEEE 802.11bd have been formed from 802.11 task group (TGbd) [10] and are shown in Table 2.2

Feature	
Radio bands of operation	5.9 GHz & 60 GHz
Channel coding	LDPC
Doppler recovery method	High frequency midambles
Sub-carrier spacing	312.5 KHz, 156.25 KHz, 78.125 KHz
Supported relative speeds	500 Kmph
FFT size	56 sub carriers
Channel bandwidth	10 MHz/20 MHz

Table 2.2: PHYs implementations in IEEE 802.11bd

The technologies that were introduced in the 802.11bd for performance enhancement include[9]:

- **Low density parity check (LDPC):** codes which are more efficient at larger payloads increase net data rates and reliability
- **Space time block coding (STBC)**: enhance reliability by enabling two diversity branches on transmitter side
- **Data Communication module (DCM)**: achieve frequency diversity by transmitting the same symbol twice over sufficiently distant sub-carriers can help boost the efficiency of block-error-rate (BLER) given the rise in modulation order. It is also used in 802.11ax.
- **Multiple input multiple output (MIMO):** transmissions that offer more bandwidth options and hence increasing the throughput
- **Multiple cyclic prefix (CP)**: durations that makes the 802.11 standards more suitable for outdoor environments by enabling scenario specific selection for inter symbol interference prevention
- **Use of midambles** : so as to get higher periodicity of channel estimations that allows better handling of high Doppler shifts as shown in Figure 2.2:

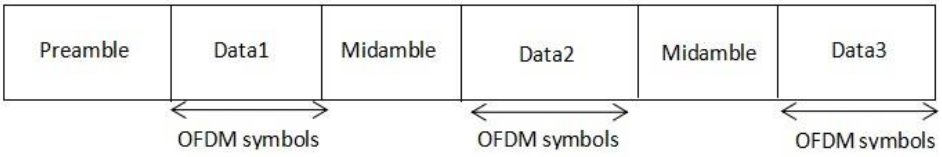

Figure 2.2: Midambles insertion for improved Channel Estimation

Note that the preamble used for estimation in the beginning of the frame for synchronization and channel estimation but can't be used again due to fast varying channels the initial channel estimate becomes outdated and there are chances of erroneous reception therefore high frequency is considered so as to avoid this scenario due Doppler shift in the channel estimation. A general comparison 802.11p and 802.11bd standard are shown blow [11].

Feature	**802.11p**	**802.11bd**
Radio bands of operation	5.9 GHz	5.9 GHz – 60Gz
Channel coding	BCC	LDPC
Re-transmissions	None	Congestion dependent
Counter measures against Doppler shift	None	Midambles
Sub-carrier spacing	156.25 KHz	156.25KHz, 312.5 KHz, 78.125 KHz
Relative speeds	252 Km/h	500 Km/h
Spatial streams	One	Multiple

Table 2.3: 802.11p and 802.11bd comparison

Although there are different features in both technologies yet they are able to co-exist where the 802.11bd is able to interoperable with IEEE 802.11p which is known as the backward compatibility .Furthermore, both technologies are able to recognize transmission modes of each other(at least one mode) and have equal channel access possibilities in co-channel scenarios .[9]

2.3 Channel Properties

This section covers the properties and factors that affect the wireless channel since they play a great role in the V2X system especially when the simulation part of this thesis depend greatly in calculations based on the channel properties. A transmitted signal generally undergoes several paths when transmitted due to reflections, diffraction and scattering this is known as the multipath propagation phenomena which have a direct impact to the Wireless channels .Another components such as the direct path, which is called Line of Sight (LOS) and the non-Line of Sight (non-LOS) paths are also described in this section. [12]

2.3.1 Line of Sight (LOS)

LoS is a type of propagation where the transmitter and receiver are in view of each other without any sort of an obstacle between them. To understand the LOS we use Friis' law that indicate that the attenuation in the received power is directly proportional to the carrier frequency and distance. taking into account the free space environment Friss law can be shown in Equation 2.1

$$P_{RX} = P_{TX} G_{TX} G_{RX} \left(\frac{c}{4\pi df}\right)^2 \qquad 2.1$$

Where

- P_{RX} is the received power
- f is the carrier frequency
- d is the distance
- G_{TX} antenna gains of the transmitter
- G_{RX} antenna gains of the receiver.
- The speed of light c is $3 \times 10^8\, m/sec.$

Friis' equation in dB is as equation 2.2 shows.

$$P_{RX\_dB} = P_{TX\_dB} + G_{TX\_dB} + G_{RX\_dB} + 20\, log\left(\frac{f}{4\pi dc}\right) \qquad 2.2$$

To apply Friis' law the distance between the transmitter (TX) and the receiver (RX) should be at least one Rayleigh distance d_r which is the dimension of the largest antenna as shown in equation 2.3 where L_a is the largest dimension of the antenna.

$$d_r = \frac{2f{L_a}^2}{c} \qquad 2.3$$

The attenuation of the LOS signal is the inverse of the Free Space Loss Factor (FSLF) in case of isotropic antennas where $G_{TX} = G_{RX} = 1$ .This attenuation is inversely proportional to the wave length ($\lambda = \frac{c}{f}$) and the distance as shown in Equation 2.4 and Figure 2.3 [13] .

$$FSLF = \left(\frac{\lambda}{4\pi d}\right)^2 \qquad 2.4$$

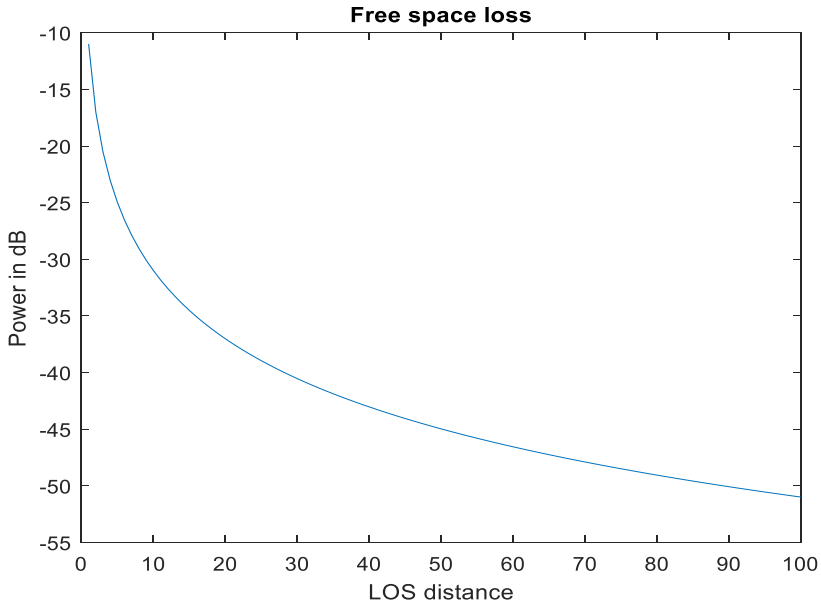

Figure 2.3: Free space loss in dB vs Distances in meters

2.3.2 Non line of sight

Non-line of sight (NLOS) is the of propagation of a signal that is obscured (partially or completely) by obstacles, thus making it difficult for the signal to pass through. Common obstacles between transmitters and receivers are tall buildings, trees, physical landscape and

high-voltage power conductors. While some obstacles absorb and others reflect the radio signal; they all limit the transmission ability of signals. In addition, electromagnetic waves (signals) can also get diffracted at the edges of these objects [12].

2.3.3 Reflection

As a wave radiates from an antenna, it broadens and disperses. If portions of the wave are reflected by smooth surface, new wave fronts appear from the reflection points.

The received power is determined by both the direction of reflection and the reflection coefficient which can be found using the two-ray ground reflection model as shown in Figure 2.4 [12].

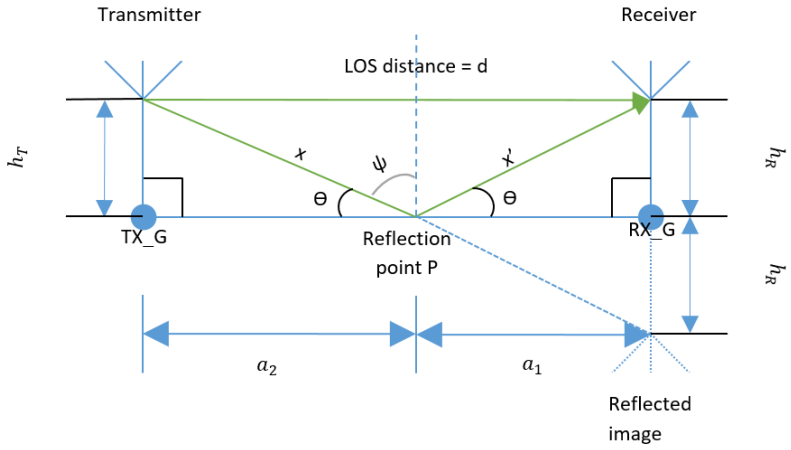

Figure 2.4: Two-ray model

The received power on the LOS path is found by equation 2.5, and the reflected power of the reflecting material is:

$$P_{ref} = P_{TX} \cdot \alpha(\Theta) \cdot G_{TX} \cdot G_{RX} \cdot \left(\frac{c}{4\pi(x + x')f}\right)^2 \qquad 2.5$$

Where

- x is the distance between the transmitter to the reflection point
- x' is the distance from the reflection point to the receiver
- $\alpha(\Theta)$ is the reflection coefficient as shown in figure 2.5

$$\alpha(\Theta) = \frac{sin\Theta - X}{sin\Theta + X} \qquad 2.6$$

- X is the material properties that caused the reflection and depend on the horizontal and vertical polarizations.

$$X_v = \frac{X_h}{\varepsilon} = \frac{\sqrt{\varepsilon - \cos^2 \Theta}}{\varepsilon} \qquad 2.7$$

The relative permittivity of the material is ε . Figure 2.6 shows the reflection coefficient for both horizontal and vertical polarization signal with the change of the angle of arrival Θ.

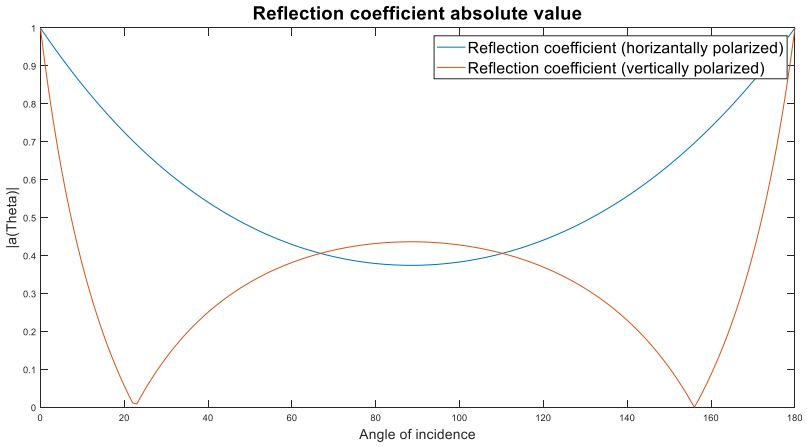

Figure 2.5: Reflection coefficient

2.3.3.1 Reflection point algorithm

From Figure 2.5 the triangle between the Transmitter position, TX_G and P positions is equal to the triangle between Receiver position, RX_G and P due to the fact that their angles are equation thus:

$$\tan\theta = \frac{h_T}{h_R} = \frac{a_2}{a_1} \qquad 2.8$$

The unit vector $\overrightarrow{V}$ is found by equation 2.9

$$\vec{V} = \frac{RX\_G - TX\_G}{\|RX\_G - TX\_G\|} \qquad 2.9$$

The distance between TX_G and RX_G is:

$$a_1 + a_2 = \|RX\_G - TX\_G\| \qquad 2.10$$

the reflection point as equation 2.11 shows.

$$P = RX\_G + \vec{V} \, . \, a_1 \qquad 2.11$$

2.3.4 Diffraction

Diffraction is the spreading of the signal around obstacles. diffraction occur at the edges of objects due to their limited size and the electromagnetic wave nature . If an object is placed between TX and RX there will be a part of the LOS power received by the receiver as shown in Figure 2.7.

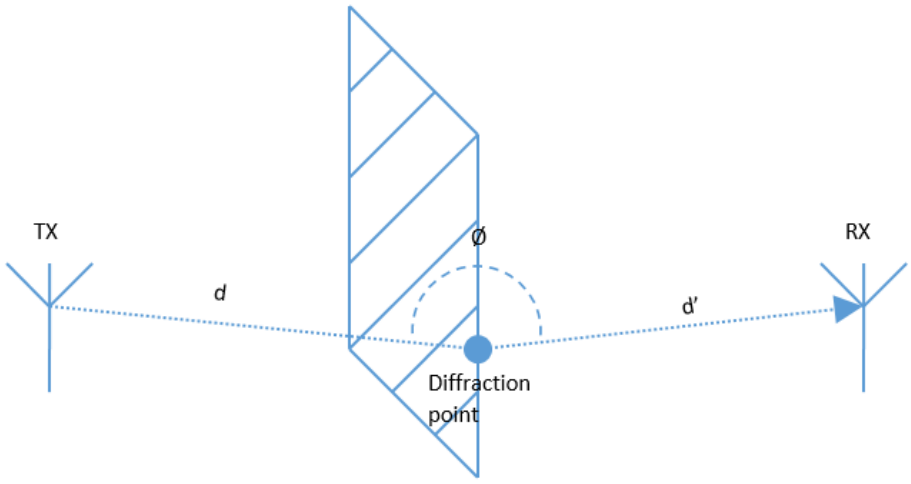

Figure 2.6: Diffraction

The diffraction coefficient β is calculated by equation 2.12.

$$\beta = \frac{\cos(y) + 1}{2} \qquad 2.12$$

Where: $y = 180^0 \ \ at \ \ 0 < Ø < 165$,

$$y = -\frac{180}{13}(Ø - 180)^o \quad at \quad 165 < Ø < 180,$$

$$y = 0^0, \quad Ø \geq 180$$

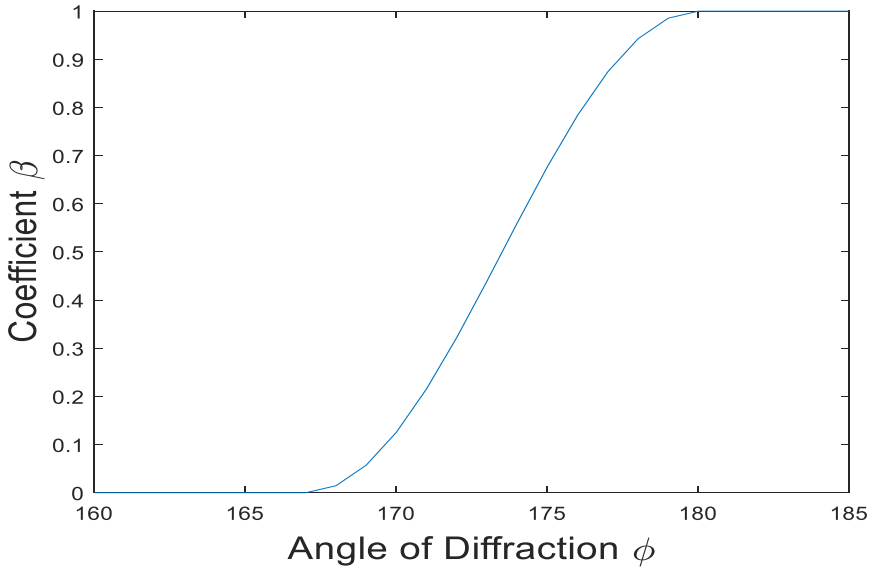

Figure 2.7: Diffraction coefficient

As the TX is moving, if the angle of diffraction is increasing the power at the receiver also increase otherwise the receiver receives portion of the power transmitted.

2.3.5 Doppler shift

Doppler shifts is the difference in frequency between the transmitted and received signal due to the movement of either the transmitter TX, the receiver RX or both. The relative

movement shifts the frequency of the signal hence causing fading which is undesirable . Therefore, the Doppler shifts when arriving from multiple components can affect the channel rapidly by making it frequency selective and this has a high impact on V2X communications. The Doppler frequency is positive when the TX and RX cars are moving toward each other and negative when moving from each other. The Doppler frequency shift f_D can be calculated as:

$$f_D = \pm \frac{|v|}{\lambda} cos(\theta) \qquad 2.13$$

Where

- λ is the wave length
- v is the TX speed in the direction of wave

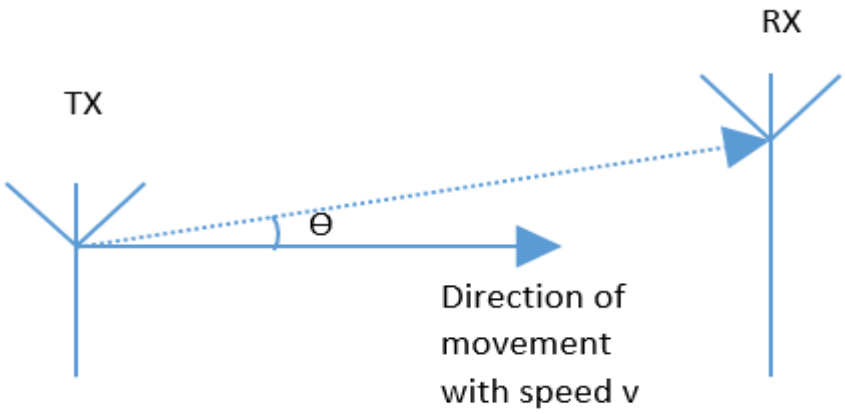

Figure 2.8: Doppler shift

The total received frequency will be:

$$f_{total} = f + f_D \qquad 2.14$$

After calculating the reflection coefficient ,diffraction coefficient and the total frequency as shown in equation 2.6, 2.12 and 2.2 respectively as well as the distance between the TX and reflection point and the distance between the receiver and the reflection point, we can calculate the LOS and non-LOS channel components, R_{LOS} and $R_{non-LOS}$ respectively, at the receiver part as :

$$R_{LOS} = \frac{c}{4\pi f_{total}} . \frac{exp(-j2\pi dc/f_{total})}{d} \quad 2.15$$

$$R_{non-LOS} = \frac{c}{4\pi f_{total}} . \alpha(\Theta). \beta . \frac{exp(-j2\pi(x+x')c/f_{total})}{x+x'} \quad 2.16$$

2.4 Channel Statistical Properties

In real environment and with the a lot of Multipath components, it is difficult describe the above mentioned properties individually therefore it is much simpler to consider the probability that the channel parameters attain a certain value .When the distance between the TX and RX cars is small the multipath components result in an attenuation of the power received which is known as small-scale fading while on larger scales and around a certain mean value is called the large-scale fading.[14]

2.4.1 Small Scale Fading Without a Direct LOS

Studies showed that the probability density function (PDF) of the received amplitude and phase resulting from an environment where there is no direct LOS with the effect of the multipath components ,can be described by the Rayleigh distribution which describes the magnitude of a complex stochastic variable with an independent and normally distributed real and imaginary parts as shown in Figure 2.10

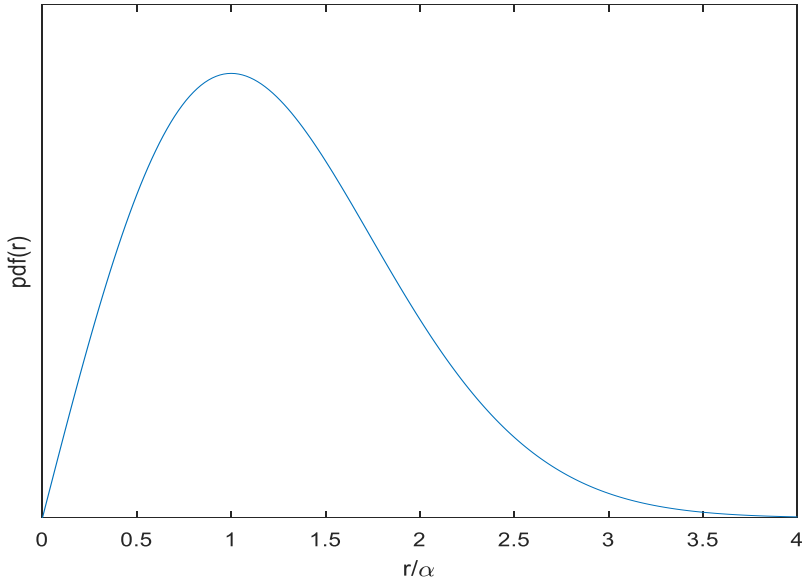

Figure 2.9: Rayleigh distribution

PDF of a normally distributed variable x with a zero is given by:

$$pdf_x(x) = \frac{1}{\sqrt{2\pi}\sigma} exp\left(-\frac{x^2}{2\sigma^2}\right) \quad 2.17$$

Where σ^2 is the variance of the normal (Gaussian) distribution.

The pdf of the received power amplitude's (r) is:

$$pdf_r(r) = \frac{r}{\sigma^2}\ exp\left(-\frac{r^2}{2\sigma^2}\right) \quad 2.18$$

And the received phase Φ distribution is uniformly distributed as:

$$pdf_\Phi(\Phi) = \frac{1}{2\pi} \quad 2.19$$

The mean square value of a Raleigh distributed random variable is:

$$\overline{r^2} = 2\sigma^2 \qquad 2.20$$

The product of both amplitude PDF and phase pPDF gives the same distribution as the Rayleigh distribution. Thus small scale fading without a dominant component is described as a Rayleigh distribution with the same statistical properties.

2.4.2 Small Scale Fading With a Direct LOS

Measurements and experiments done in an environment with a TX, RX and MPC, with a direct LOS (dominant component) between TX and RX, showed that the Probability Density Function (PDF) of the received amplitude and phase, behaves the same way as the Rician distribution.[15] A Rician distribution, shown in Figure 2.11, describes the magnitude of a complex stochastic variable whose real part is non-zero mean, due to LOS, Gaussian distributed and the imaginary part is zero mean Gaussian distributed.

The PDF of the amplitude (r) is same as the Rice distribution:

$$pdf_r(r) = \frac{r}{\sigma^2}.exp\left(-\frac{r^2 + A^2}{2\sigma^2}\right).I_0\left(\frac{rA}{\sigma^2}\right) \qquad 2.21$$

Where I_0 is the first kind Bessel function, zero order [16], A is the amplitude of the dominant component (LOS) and σ^2 is the variance.

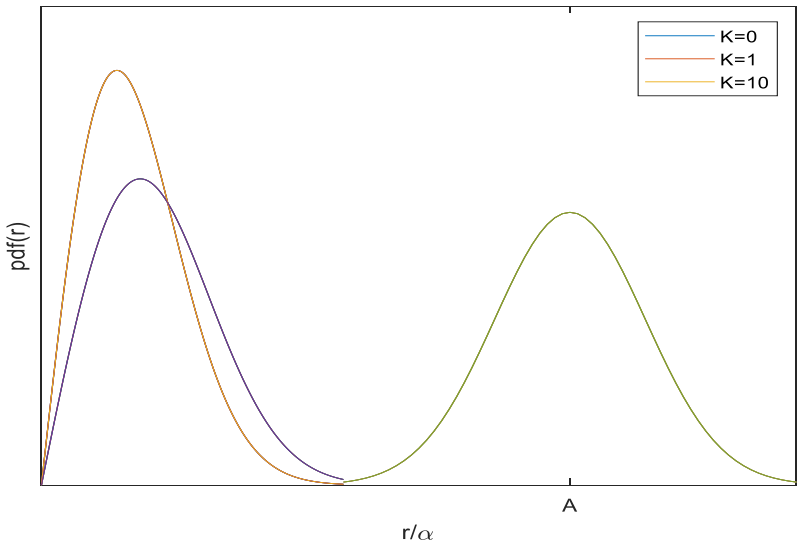

Figure 2.10: Rician distribution

The mean square value of a Rice distributed random variable (received amplitude r) is:

$$\overline{r^2} = 2\sigma^2 + A^2 \qquad 2.22$$

The rice factor K is the ratio between the line of sight (LOS) component A and the non-LOS component.

$$K = \frac{A^2}{2\sigma^2} \qquad 2.23$$

Phase PDF is given by [17]:

$$pdf_{\Phi}(\Phi) = \frac{1 + \sqrt{\pi K}.exp\left(kcos^2(\Phi)\right).cos(\Phi).(1 + \text{erf}(K.cos(\Phi)))}{2\pi \exp(K)} \qquad 2.24$$

Where erf(x) is the error function calculated as [16]:

$$\text{erf}(x) = \left(\frac{2}{\pi}\right) \int_0^x exp(-t^2)\, dt \qquad 2.25$$

As the K factor goes to zero (losing LOS component) the PDF distribution becomes similar to the Rayleigh distribution as shown in Figure 2.11

2.4.3 Large Scale Fading

The small-scale field strength averaged over a larger spatial scale, varies due to the shadowing of the LOS and non-LOS components by other objects.

Many experiments showed that the latter averaged field strength P plotted on a logarithmic scale gives a Gaussian distribution with mean μ . This distribution is known as log normal with PDF as[17]:

$$pdf_P(P) = \frac{20/ln(10)}{P.\sigma_P}.exp\left(-\frac{(20log_{10}(P)-\mu_{dB})^2}{2.\sigma_P^2}\right) \quad 2.26$$

Where σ_P^2 is the variance and μ_{dB} is the mean value expressed in dB.

2.4.4 Additive White Gaussian Noise

When the signal is received in the RX, it will be affected by the attenuation from the different MPC. In addition, there is the noise that effects the signal and this can be caused either by the thermal noise, which comes from the TX and RX temperature, the man-made noises, for example other electrical devices which emits over a large bandwidth, or the noisy TX and RX components (ex. Amplifiers and mixers) [18].

All of the types of noise mentioned above can be seen as uniformly distributed; since the central limit theory indicates that having many random processes summed together, gives a Gaussian (random) distribution. The additive white Gaussian model (AWGN), has a uniform power on the frequency domain, thus the name white, which refers to the color white with the uniform emissions. AWGN is Gaussian, since the amplitudes of the noise is supposed to be normally distributed as the central limit theory indicates [20]]

2.4.5 Doppler Spectrum

What was explained previously about the Doppler Effect is applied in the simple scenario when you have one direction of movement and one signal e.g. coming from LOS. In a more complicated environment (reality), the RX will be receiving many signals from several MPC with different directions and projected speeds, hence different Doppler shifts. These variations are captured on what's called the Doppler spectrum [21].

The received power spectrum as a function of the angle between the speed direction and the signal wave, depicted as Θ is :

$$S(\theta) = \Omega[pdf_\theta(\theta)\, G(\theta) + pdf_\theta(-\theta)\, G(-\theta)] \qquad 2.27$$

Where Ω is the mean power of the arriving wave, $G(\theta)$ is the antenna gain, $pdf_\theta(\theta)$ represents the distribution of the incident waves in terms of the arriving direction and putting into account that the waves arriving from Θ and -Θ have the same Doppler shifts.

By using Jacobean theorem, we can transform the variable Θ to f_D, which is dependent on the velocity ($|v|\, cos(\theta)$), by the following equation:

$$t = \left|\frac{d\theta}{df_D}\right| = \left|\frac{1}{\frac{df_D}{d\theta}}\right| = \frac{1}{\left|\frac{v}{c}\, f\, sin(\theta)\right|} = \frac{1}{\sqrt{v_{max}^2 - {f_D}^2}} \qquad 2.28$$

Where c is the speed of light and $v_{max} = f_{D\,max} = fv/c$.

So,

$$S_D(f_D) \qquad 2.29$$

$$= \begin{cases} S(\theta).\dfrac{1}{\sqrt{v_{max}^2 - {f_D}^2}} & for - v_{max} \le f_D \le v_{max} \\ 0 & otherwise \end{cases}$$

Depending on the angular distribution and the antenna patterns different models of the Doppler spectrum can be noticed. The simplest model is known as the Jake's spectrum (bathtub). In the latter model the angular distribution is assumed to be uniformly distributed with

$$pdf_\theta(\theta) = \frac{1}{2\pi} \qquad 2.30$$

Hence the power spectrum becomes:

$$S_D(f_D) = \frac{\Omega\, G(\theta)}{\pi\sqrt{v_{max}^2 - {f_D}^2}} \qquad 2.31$$

Assuming a dipole antenna with gain $G(\theta)$ =1.5 the power spectrum can be seen in Figure 2.12 taking the bathtub shape.

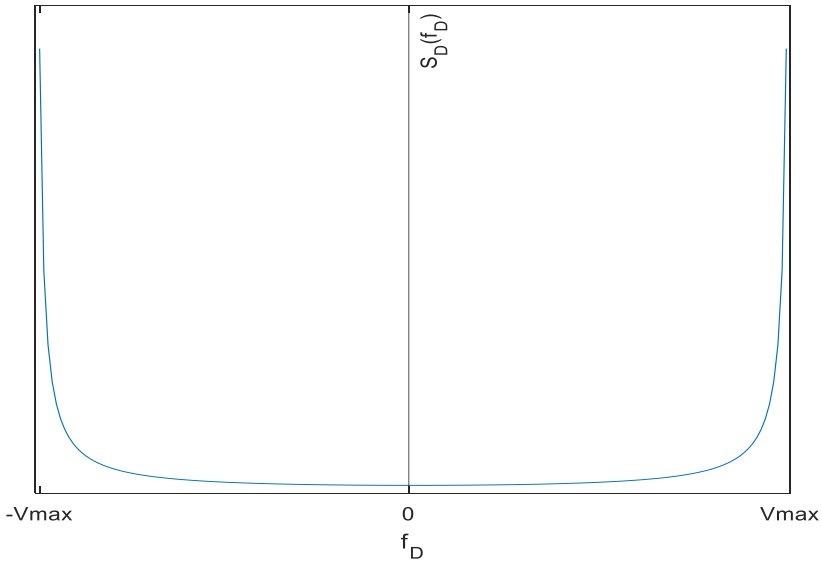

Figure 2.11: Jake's Doppler Spectrum

If the non-zero values of $S_D(f_D)$ are in the range of $f_{min} \leq f_D \leq f_{max}$ and $f_{min} = -f_{max}$ the Jake's spectrum is called symmetric Jake's as shown in the figure above. But in the other hand if $f_{min} \neq -f_{max}$ the Jake's spectrum becomes asymmetric with the power spectrum [18]:

$$S_D(f_D) = S(\theta).\frac{A_{aj}}{\sqrt{v_{max}^2 - {f_D}^2}} \quad , \qquad 2.32$$

$$for - v_{max} \leq f_{min} \leq f_D \leq f_{max} \leq v_{max}$$

Where:

$$A_{aj} = \frac{\pi}{\sin^{-1}\left(\frac{f_{max}}{f_D}\right) - \sin^{-1}\left(\frac{f_{min}}{f_D}\right)} \qquad 2.33$$

The Jake's spectrum is the most commonly model used to model the Doppler spectrum. Aulin's model, which limits the non-zero values of the Jake's Doppler spectrum, and the Gaussian Doppler spectrum model are examples of alternative models [21].

2.5 Channel Models

Channel modeling is the calculation and estimation of all the characteristics and factors that affect the propagation of the signal from the transmitter to the receiver . The Channel model types are Stochastic model and deterministic model. Due to the importance of low latency in a V2X system , it's necessary to have a good knowledge of the propagation channel since it is vital to design, evaluate and optimize the future V2X applications[22].

2.5.1 Stochastic models

BY a Stochastic models we mean the models that have some inherent randomness. The same set of parameter values and initial conditions will lead to an ensemble of different outputs. In large areas the stochastic models don't determine the exact location's impulse response since it depends in the PDF of the channel impulse .An example of the stochastic model is the Rician model, which was explained in the statistical description section. These types of models comes in handy when designing and comparing systems.

2.5.2 Deterministic models

Deterministic models also called site-specific models rely on the geographical data of a wireless system environment which require a great mathematical effort to obtain the impulse response. Approximations are solved using Maxwell's equation and high-frequency approximation Deterministic models proved to be very useful in system planning and deployment. Examples of deterministic models are:

- **Ray launching :** which depend in the emission of several rays from the transmitter in different directions then following each launched ray and considering attenuation resulting from reflection , free-loss or diffraction
- **Ray tracing:** depend on gaining the description of MPC by computing the attenuation of the pre-determined rays from the transmitter to the receiver. Ray tracing fail to perform in areas with high reflections and scattering.

CHAPTER 3

Methodology

In this section the methods and procedures made so as to Understand and evaluate the two WLAN based V2X technologies are described .The procedure can be divided into three steps starting by the creation of the channel model of a certain scenarios using the deterministic approaches then the second step is calculation of the channel impulse response using two different methods that will be further explained In this chapter. The last step is the filtering of both the IEEE 802.11P and 802.11Bd separately by the created channel model and evaluate the performance using a V2X simulator.

3.1 Channel Model Creation

In this step a simulator called Unity 3D Game Engine was used so as to create a vehicular environment by using real geographical locations and coordinates. The vehicular environment was created using the following steps:

- Obtaining geographical coordinates and information using Google Earth.
- Creation of the cars that represent our transmitter and receiver and making roads walk-able for the cars.
- Adding colors and objects to enhance the environment and making it look real as shown in figure 3.1.
- Managing surrounding buildings so as to be capable of reflecting signals.
- Sending the LOS path and the N-LOS path signals from the moving TX car to the stationary RX car as shown in figure 3.2.
- The TX calculates the reflection points from nearby buildings and tracing these rays to check either they reach the RX car or no. This is done using the reflection calculation in section 2.2.3.1.

Figure 3.1: Unity's channel environment

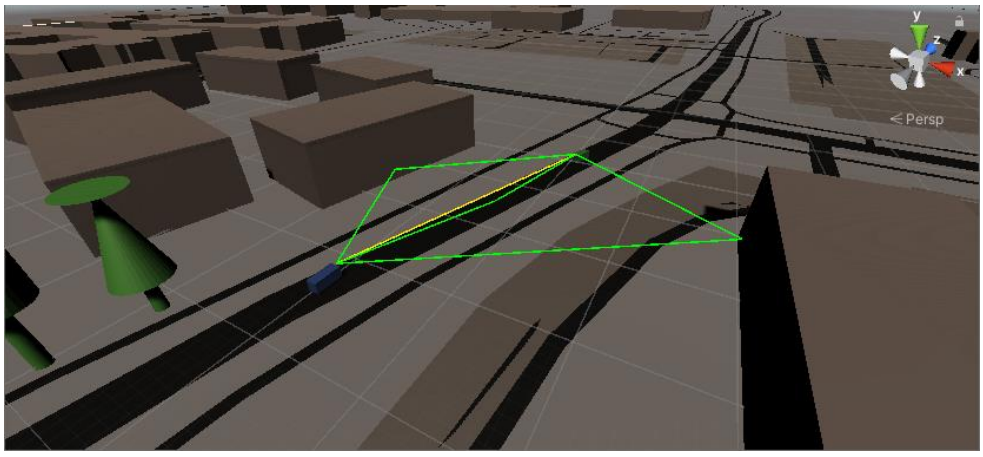

Figure 3.2: LOS and non-LOS components

The steps mentioned above were executed so as to get the values of :

- Incidence angles
- Diffraction angles
- Doppler shifts angle
- Distances of both LOS paths and non-LOS paths

The abovementioned calculations are used furthermore so as to get the channel impulse response . The channel description at every time instant h_i is described by LOS channel component R_{LOS} and the non-LOS component $R_{non-LOS}$ components which are obtained from equations 2.15 and2.16, which will include the LOS path and other non-LOS paths:

$$h_i = [R_{LOS_0}, R_{non-LOS_1}, R_{non-LOS_2}, R_{non-LOS_3} \dots R_{non-LOS_N}] \quad 3.1$$

3.1.1 Reflection point calculations

To calculate the reflection point, the TX uses ray tracing to determines the vertices of the objects within a certain radius around it and concentrates only In the ones that reflect the signals towards the RX .Figure 3.3 shows that X1,X2,X3 and X6 have the same normal vector hence they are on the same surface.

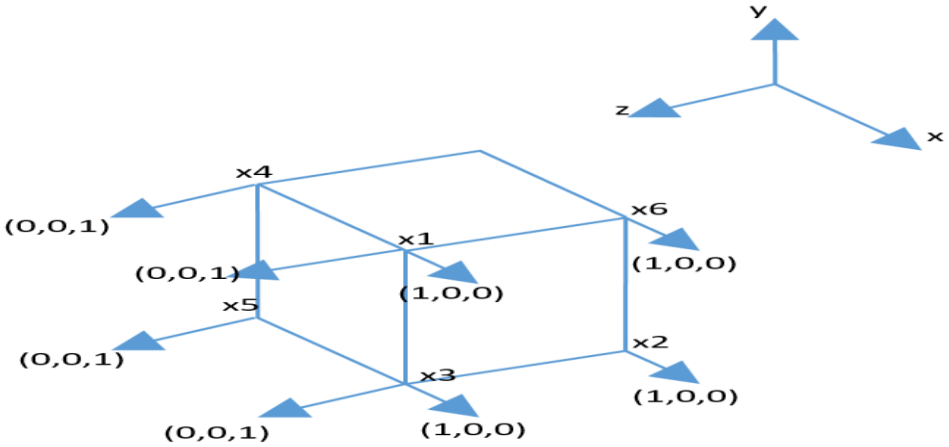

Figure 3.3: Building Vertices

Then obtaining the position where the reflection happens (P) and check if it is located between v1 and v2 (wall vertices.) as shown in Figure 3.4

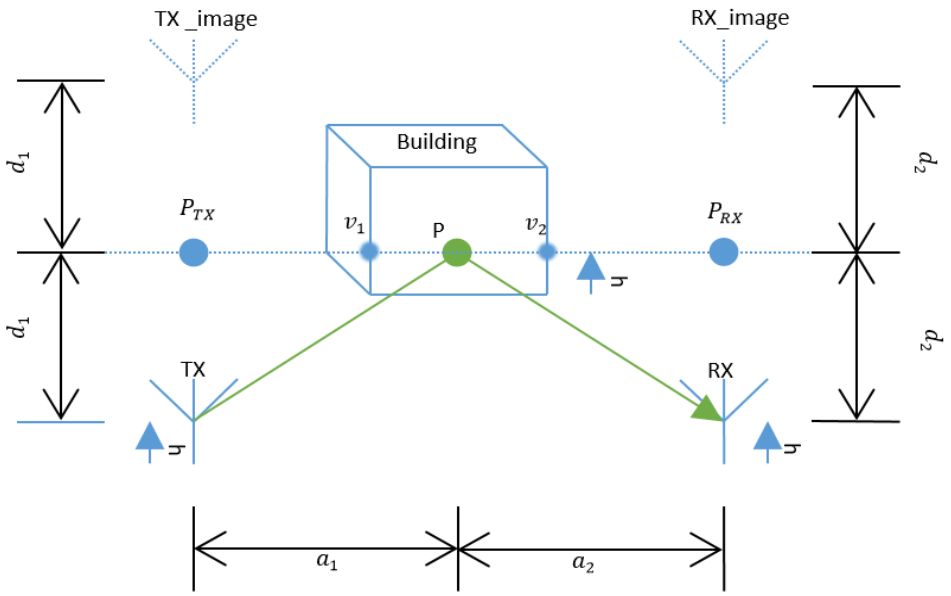

Figure 3.4: Reflection point

Given the exact Tx and Rx locations as well as the antenna height h and the building's vertices , p can be found using 3.1 and calculations from section 2.3.3

$$P = P_{RX} + \vec{V}.a_2 \quad 3.2$$

Where $\vec{V} = \frac{P_{RX}-P_{TX}}{\|P_{RX}-P_{TX}\|}$, Figure 3.4 is used to find P_{RX} and P_{TX} .To get $\vec{r}$(vector between RX_L and v_2)

$$\vec{r} = v_2 - RX_L \quad 3.3$$

Hence the distance between v_2 and RX_L:

$$\boldsymbol{d_2 = |\vec{r}|.\cos(\theta)} \quad 3.4$$

Θ is the angle between the normal vector of $\overrightarrow{v_2}$ and $\vec{r}$

Since the vector between the RX and its image is 2 d_2 RX image position is:

$$RX_{image_L} = RX_L - 2\, d_2.\overrightarrow{v_2} \quad 3.5$$

Therefore

$$P_{RX} = \frac{RX_L + RX_{image_L}}{2} \quad 3.6$$

While

$$P_{TX} = \frac{TX_L + TX_{image_L}}{2} \quad 3.7$$

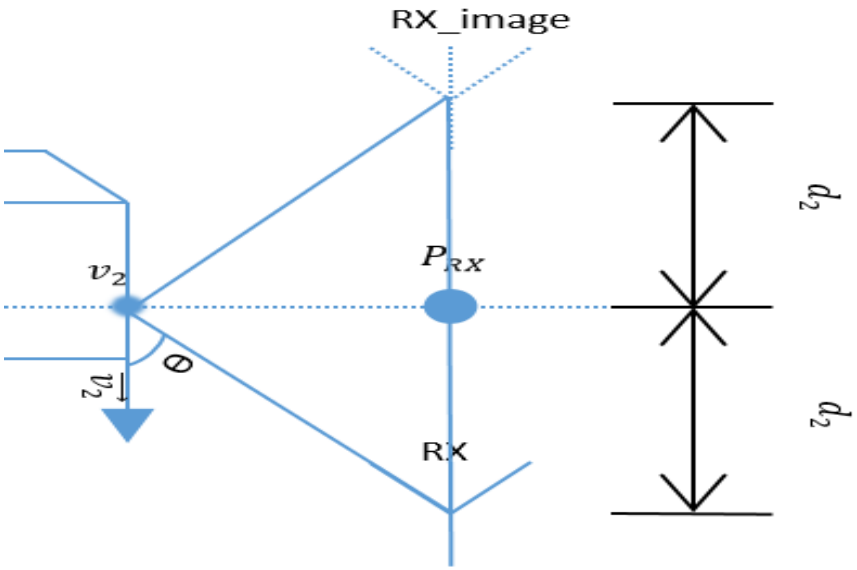

Figure 3.5

After finding P_{RX} *and* P_{TX} points on Figure 3.5, P in 3D can be calculated as the following:

$$P = P_{RX} + \frac{P_{RX} - P_{TX}}{\|P_{RX} - P_{TX}\|}.a_1 = P_{RX} + \frac{P_{RX} - P_{TX}}{1 + d_2/d_1} \quad 3.8$$

Since, $a_1 = \frac{\|P_{RX} - P_{TX}\|}{1 + d_2/d_1}$ by solving equations 2.8 and 2.10. Where h_r and h_t represents d_2 and d_1 respectively in this case.

3.2 Channel Impulse Response (CIR) calculations

The simulator results previously obtained undergoes further calculations in order to get the CIR which is characterized by three parameters which are Delay , Power and Doppler frequency. The calculations made to obtain these results were done by using MATLAB. Two methods were used to find the CIR:

3.2.1 Deterministic and Stochastic Method

The data from the unity program is calculated at every time interval i.e. no channel data have been stored between these intervals therefore to improve the channel description and compensate for the lack of data between every time interval we use the v2x simulator that create different stochastic channel models in MATLAB based on Rician and Rayleigh channel models. The V2X simulator is an open source code with a variety of functions that represent real-measurements and experiments made before for different V2X scenarios. V2X simulator have another use which is described in the last step.

3.2.1.1 Rician and Rayleigh channel model Simulation

These models need the Doppler shift f_{D_t} (which is calculated for the LOS as in equation 2.13 and N is the number of the fading paths) and the delays of each path τ calculated as the speed of light divided by the total propagation distance as shown below:

$$\tau_i = [\tau_{LOS_0}, \tau_{non-LOS_1}, \tau_{non-LOS_2}, \tau_{non-LOS_3} \dots \tau_{non-LOS_N}] \quad 3.9$$

$$and\ f_{D_i} = [\, f_{D_{LOS_0}},\, f_{D_{non-LOS_1}},\, f_{D_{tnon-LOS_2}},\, f_{D_{tnon-LOS_3}} \dots\ f_{D_{non-LOS_N}}]$$

To calculate the non-LOS Doppler shift we use the same equations used for LOS but considering the velocity to the direction of the reflection point (or RX_image in Figure 2.16); not the RX direction as in the LOS situation.

To simulate the Rayleigh and Rician channel models in MATLAB we assumed that the power and Doppler spectrum and power delay profile are separable which is known as the of band-limited discrete multipath propagation models [23].The output of the channel y_t is:

$$y_i = \sum_{n=-N_2}^{N_1} x_{t-n}.g_n \quad 3.10$$

$$g_n = \sum_{i=0}^{N} \alpha_i.sinc\left(\frac{\tau_i}{T_s} - n\right) \quad 3.11$$

Where x_t are input samples , g_n are the tap weights , T_s is The input sampling time

The uncorrelated complex path gains α_i is given by

$$\alpha_i = \sqrt{\Omega_i}.\left[\frac{z_i}{\sqrt{K_i+1}} + \sqrt{\frac{K_i}{K_i+1}}.e^{2\pi f_{D_{LOS_0}}t+\theta}\right] \qquad 3.12$$

$$z_i(t) = \mu_{in_i}(t) + j.\mu_{Q_i}(t) \qquad 3.13$$

Where Ω_i is the mean value of the h_i values, θ is the phase of the LOS path K_i is the Rician factor and z_i contains the in-phase μ_{in} and quadrature μ_Q components and are found by:

$$\mu_i(t) = \sqrt{\frac{2}{S_i}}\sum_{n=1}^{S_i}\cos(2\pi f_{D_{i,n}}t + \theta_{i,n}) \qquad 3.14$$

Where S_i is the number of sinusoids needed so as to model a single path, t is the fading time and $\theta_{i,n}$ is the phase of the nth component of a certain path.

$$f_{D_{i,n}} = f_{D_{max}}\cos\left(\frac{\pi}{2S_i}\left(n-\frac{1}{2}\right)+\alpha_{i,0}\right) \qquad 3.15$$

Where:

$$\alpha_{i,0} \triangleq \begin{cases} \frac{\pi}{4S_i}.\frac{i}{N+2} & ,if\ \mu = \mu_{in} \\ -\frac{\pi}{4S_i}.\frac{i}{N+2} & ,if\ \mu = \mu_Q \end{cases} \qquad 3.16$$

Equation 3.15 and 3.16 represent a Jake's Doppler spectrum model.

Note that the Doppler spectrum of each path can be structured as an Asymmetric Jake's spectrum as described in the theory part and by using equation 2.32 and 2.33, in which f_{min}

and f_{max} can be seen as the minimum and maximum Doppler shifts of the given paths respectively [24].

3.2.2 Direct method

In this method the CIR is described using the Tapped Delay line model for wide band signals considering the fact that the data obtained from unity simulator have delays between time intervals.[19],thus the CIR $h(t,\tau)$ becomes:

$$\boldsymbol{h(t,\tau) = a_0\delta(\tau-\tau_0) + \sum_{i=1}^{N} c_i(t)\delta(\tau-\tau_i)} \quad 3.17$$

Where a_0 is the LOS component

$c_i(t)$ is the complex zero mean Gaussian process associated with Doppler spectrum.

The Rayleigh fading model is an example of the tapped delay line model and it is commonly used to exhibit delay dispersions by using a stochastic fading channel is known as a two-path channel or two delay channel .

3.2.2.1 Channel Matrices

Are used for modeling double-directional, time-variant and complex channel frequency transfer functions of different multipath components such as different reflections from LOS, road and NLOS objects. Channel matrices use transfer functions so as to store all the different Multipath Components (MPC) that a vehicle encounter when moving from initial position to reflection point and to the destination . These MPC are modeled using the transfer function as seen in Figure 3.5

$$H(k) = ((\frac{\lambda}{4\pi d})*a_{LOS})*(e^{j2\pi(fk+fd\_LOS)*\frac{d}{c}}) + ((\frac{\lambda}{4\pi d_1})*a_{road})*(e^{j2\pi(fk+fd\_road)*\frac{d_1}{c}}) +$$

$$((\frac{\lambda}{4\pi d_3})*a_{NLOS1})*(e^{j2\pi(fk+fd\_NLOS1)*\frac{d_3}{c}}) + ...$$

Figure 3.5: Transfer function

Where

- c is the speed of light (3x10^8 m/s)
- $a_{LOS}$is the amplitude of Line of sight (LOS)
- fd_LOS is the Doppler shift of LOS

- fk is the sum of frequency band and sub carriers (k = 64)
- a_{road} is amplitude of road + ground reflection
- fd_road is the Doppler shift road reflection
- $a_{NLOS1}$is the amplitude of Non Line of Sight reflection object (non-LOS)
- Δf is the sub carrier spacing of IEEE 802.11p (156.25khz)
- F is frequency band of .11p (5.9 GHz)
- d1, d2, d3 are the distances of LOS, road and non-LOS reflections.

These time instances are plotted to get the channel impulse response to see the performance of the vehicle until it approaches the destination. The time domain is obtained by taking Inverse Fast Fourier Transform (IFFT) of the transfer function in frequency domain.

3.3 Performance Measurement

After the creation of the channel model and the calculation of the CIR by either of the two methods described previously, the data is introduced to the V2X simulator so as to initiate the performance measurement for each of the IEEE signal models (802.11p and 802.11bd) separately by the following steps:

- Calculation of the average SNR value at each time instant for a fixed noise floor of -100dBm.
- Filtering the selected signal model to be tested with the created channel
- Addition of AWGN and phase average SNR value of the selected signal model.
- After the channel estimation and the determination of errors, the PER and throughput is calculated for every time instant.
- The simulator detects the synchronization point of the signal, do channel estimation, get the received packets

This process is repeated for every time instant using Monte-Carlo iteration technique to get more accurate results. The performance of these signal models is measured by the PER and throughput. MEX files should be used for high level TX and RX functions so as to enhance the simulation performance.

3.3.1 Average Packet error rate

The Packet Error Ratio (PER) is the number of incorrectly received data packets divided by the total number of received packets. A packet is declared incorrect if at least one bit is erroneous. Factors affecting PER:

- Invalidity of the synchronization point after separating it from the preamble pilot.
- Invalidity of the even parity check of the first part of the received bits, after channel calibration and decoding
- Decoded length of signal is not a valid number
- Coding and modulation scheme determined from the first four bits is not valid.
- Payload length or the number of OFDM symbols is not the same as the stored values
- Data error

For a better performance measurement the average PER is calculated for different iterations (N):

.

$$avgPER = \frac{\sum_{i=1}^{N} PER(i)}{N} \qquad 3.18$$

3.3.2 Throughput

It is the actual amount of data that is successfully sent/received between the TX and RX.

The simulator assigns an efficiency factor (eff) and is set to 1 in case of calculating the throughput for the IEEE 802.11p but for the IEEE 802.11bd signal model this value is dependent on the mid-amble period (mid) where eff will be:

$$eff = \frac{mid}{mid + 1} \qquad 3.19$$

And then the average throughput in Megabits per seconds (Mbps) can be found from:

$$\text{avg throughput} = (1 - \text{avgPER}) * D \qquad 3.20$$

Where:

$$D = \frac{eff.N_{dsc}.dbps.bpscs}{8.cbps} \qquad 3.21$$

And N_{dsc} is number of data subcarriers, bpscs is the number of bits per modulation symbol, cbps and dbps are the number of the coded and decoded bits per Subcarrier respectively.

CHAPTER 4

Results

This chapter discuss the outcome of the simulations and procedures used so as to evaluate and measure the performance of the IEEE 809.11p and 809.11bd The results obtained are :

- Unity game engine result
- Channel impulse response results with the two different ways
- The signal models performance based on The V2X stochastic real time channel measurements
- The signal models performance based on The deterministic channel we created

4.1 Unity Game Engine Result

Using the Unity 3D game engine an Urban scenario was created as shown in Figure 4.1 and after the creation of the vehicular environment as discussed in section 3.1 the following assumptions were made for the simulation:

- The scenario was created in free space and noise component was neglected.
- Isotropic antennas were used for both the TX and RX cars with a gain of 0db.
- The TX car moving with a speed of 12.6 km/h while the RX car is static.
- Transmitted power is30dbm with a carrier frequency of 5.9 GHz.
- Minimum Number of components per time instant to be received at the Rx antenna are two components (LOS and Non-LOS components) while the maximum number of components to be received per time instant are four (LOS , Non-LOS components road reflection component and buildings reflection components).
- Roads permittivity is 3.5 while that of the buildings is 5.
- Uncorrelated Doppler and delay contributions (WSSUS)

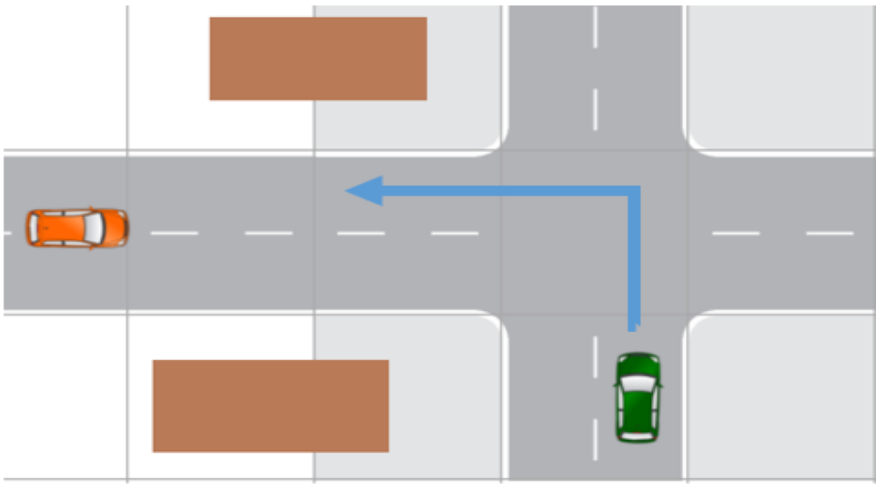

Figure 4.1: Unity's Urban LOS scenario

The results of the simulation represent the incidence angles, diffraction angles, Doppler shifts angle and the distances of both LOS paths and non-LOS paths but note that these calculations are made for every time instant that's why they are stored in a comma separated values (CSV) file so as to be introduced to MATLAB and calculate the CIR .However, the power received by the RX car is shown in Figure 4.2

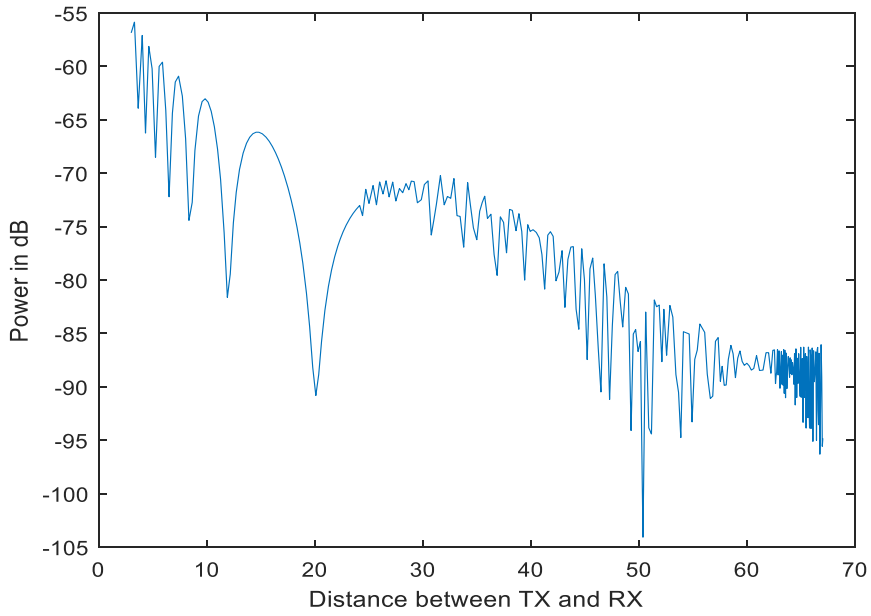

Figure 4.2: Received power

The variation in the received power shown above is due to the reflection of the transmitted signals from the road and surrounding buildings but as the distance between the TX and RX decrease the power fluctuation decrease where the LOS path occur and reflections are only from the road.

4.2 Channel Impulse Response Results

The calculations for the CIR are done in MATLAB using the data from unity program .As described in section 3.1 , we have two methods for calculating the CIR and their results are shown below.

4.2.1 Deterministic and Stochastic Method

By applying the formula in 3.17 we get the CIR or the channel description as shown in Figure 4.3 that is described by the time, delay and amplitude of the signal.

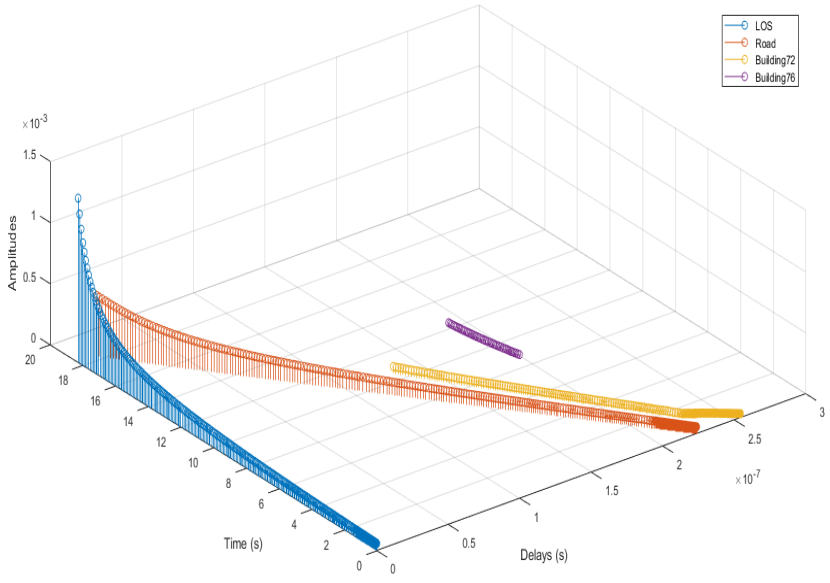

Figure 4.3: Discrete channel impulse response

The figure above shows how the distance between the TX and RX affect the CIR since the attenuation is decreased as the vehicles are close to each other .And since the distance is decreasing when the TX approaches the RX ,the Doppler shift values are positive.

4.2.2 Direct Method

Here the CIR is described by the both the frequency and time domain where the frequency impulse response is obtained by using the transfer function of LOS, road, and buildings components for each time instant using Figure 3.8 as shown in Figure 4.4

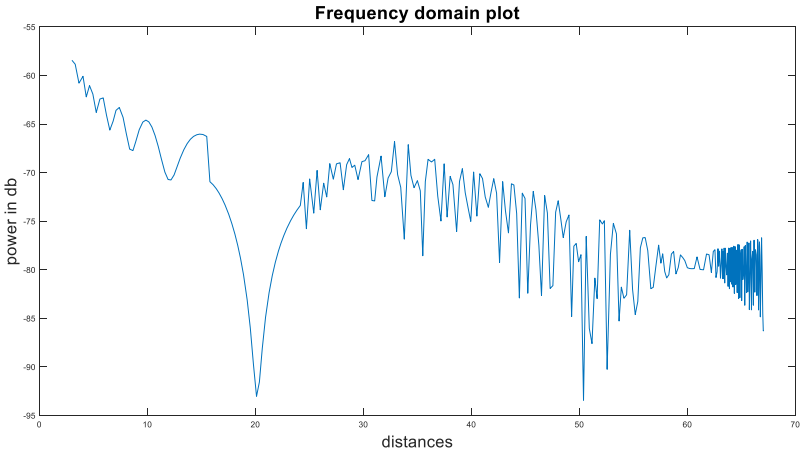

Figure 4.4: H(f) vs LOS Distance

The Inverse Fast Fourier Transform of the above frequency impulse response results the time domain plot of the CIR as shown below

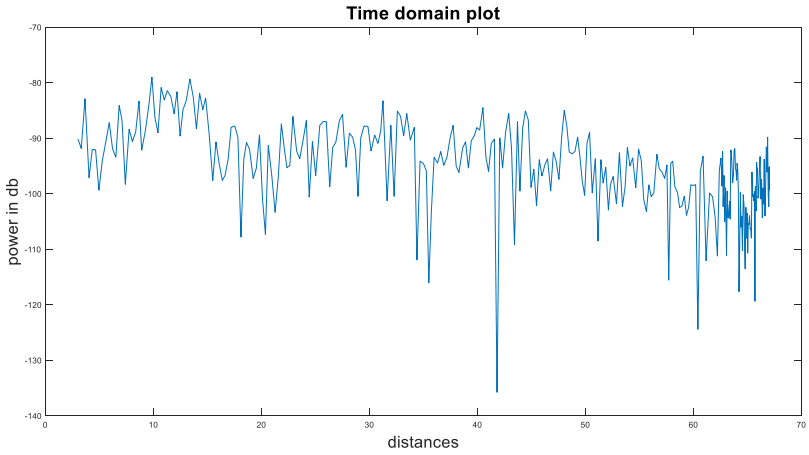

Figure 4.5: H(t)

4.3 The signal Models Performance

The above mentioned results were just describing the simulated deterministic channel model of the scenario created in Unity i.e. the input data needed for channel creation and signal transmission. However, the process of the channel creation and performance of the signal models assessment is simulated using the V2X simulator which can also provide us with data of different scenarios and stochastic measurements based on experiments done before and stored in MATLAB. [22]

4.3.1 Stochastic Channel From Real Measurements

To simulate the Signal models using the V2X simulator, three different scenarios were used each with different values for the Power, delay and Doppler .The coding and modulation schemes used in the simulations are shown in Table 4.1 with SNR values ranging from 0-25 dbs.

MCS value	Coding rate	Modulation type
0	½	BPSK
1	¾	BPSK
2	½	QPSK
3	¾	QPSK
4	½	16-QAM
5	¾	16-QAM
6	2/3	64-QAM
7	¾	64-QAM

Table 4.1: Modulation and Coding Schemes for Stochastic measurements

The scenarios used in V2X simulator are:

Urban approaching LOS: Two cars moving towards each other at a maximum speed of 119km/h on average.

- Input parameters:

	Tap1	Tap2	Tap3	Tap4
Power	0dB	-8dB	-10dB	-15dB
Delay	0ns	117ns	183ns	333ns
Doppler	0Hz	236Hz	-157Hz	492Hz

Table 4.2: Urban approaching LOS parameters

- 802.11p performance:

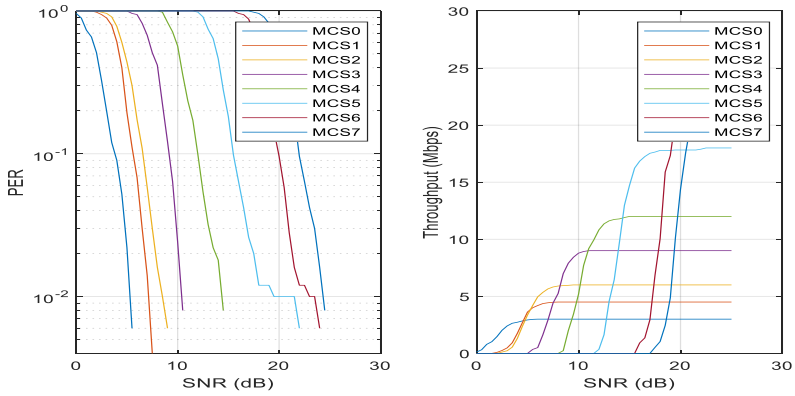

Figure 4.6: Performance of 802.11p signal model on Urban LOS channel

- 802.11bd performance (4 mid-ambles period):

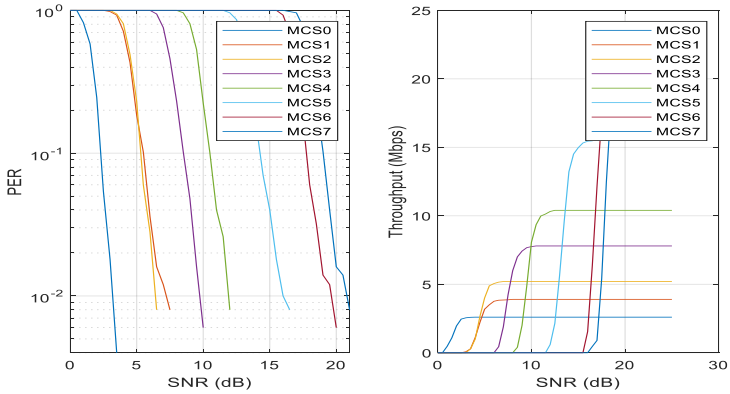

Figure 4.7: Performance of 802.11bd signal model (4 mid-amble period) on Urban LOS channel

- 802.11bd performance (8 mid-amble period) :

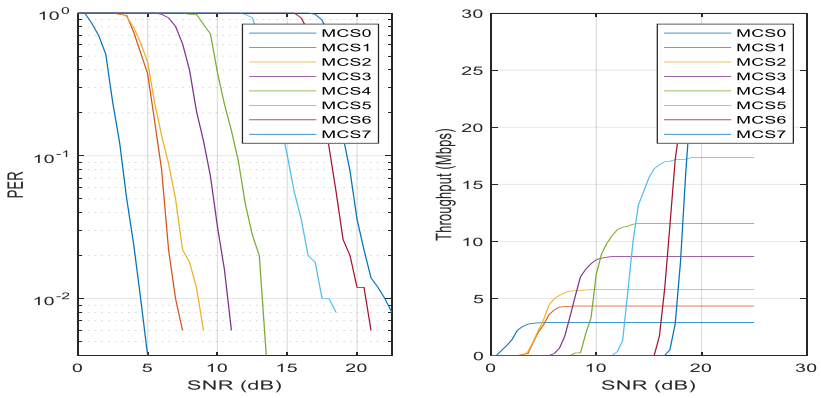

Figure 4.8: Performance of 802.11bd signal model (8 mid-amble period) on Urban LOS channel

Rural LOS channel: two cars in an open environment one moving with a speed of 144km/h and the other is stationary.

- Input parameters:

	Tap1	Tap2	Tap3
Power	0dB	-14dB	-17dB
Delay	0ns	83ns	183ns
Doppler	0Hz	492Hz	-295Hz

Table 4.3: Rural LOS parameters

- 802.11p performance:

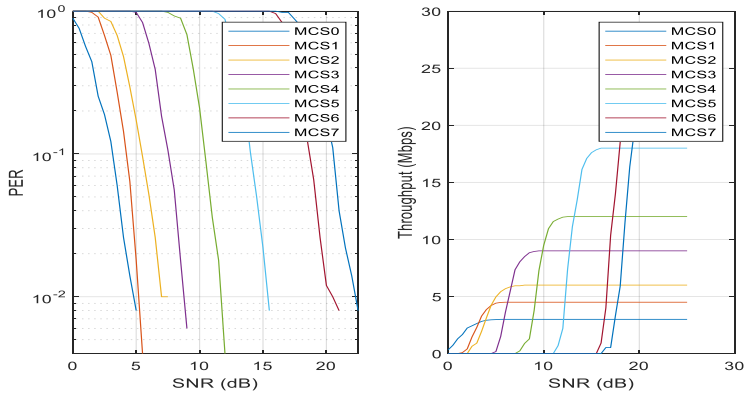

Figure 4.9: Performance of 802.11p signal model on rural LOS channel

- 802.11bd performance (4 mid-amble period) :

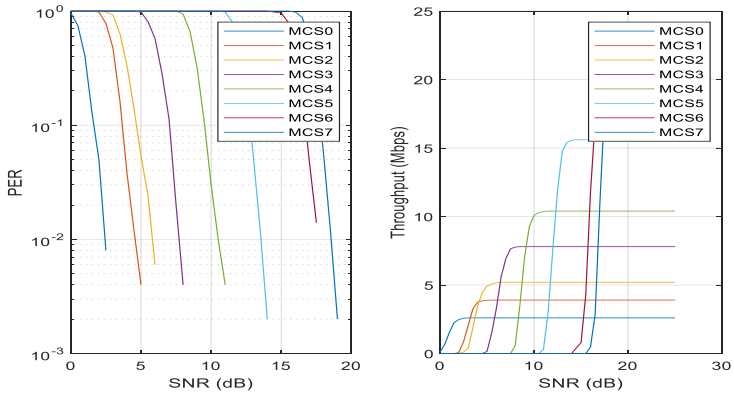

Figure 4.10: Performance of 802.11bd signal model (4 mid-amble period) on rural LOS channel

- 802.11bd performance (8 mid-amble period)

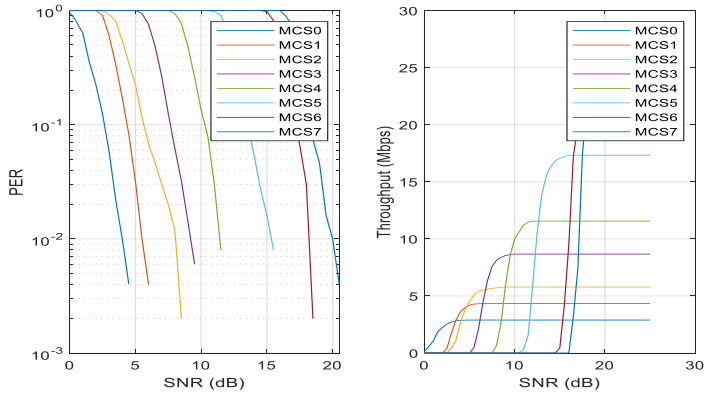

Figure 4.11: Performance of 802.11bd signal model (8 mid-amble period) on rural LOS channel

.

Street crossing non-LOS: two cars in an Urban environment moving towards an without a direct LOS at the beginning t with a maximum speed of 126km/h [19]

- Input parameters:

	Tap1	Tap2	Tap3	Tap4
Power	0dB	-3Db	-5dB	-10dB
Delay	0ns	267ns	400ns	533ns
Doppler	0Hz	295Hz	-98Hz	591Hz

Table 4.4: Crossing non-LOS parameters

- 802.11p performance:

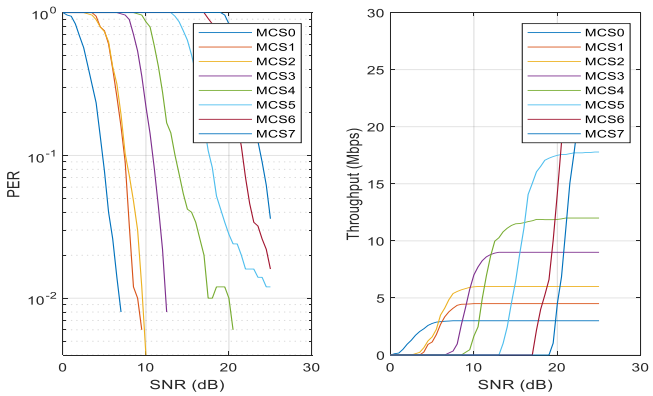

Figure 4.12: Performance of 802.11p signal model on the crossing channel

- 802.11bd performance (4 mid-amble period):

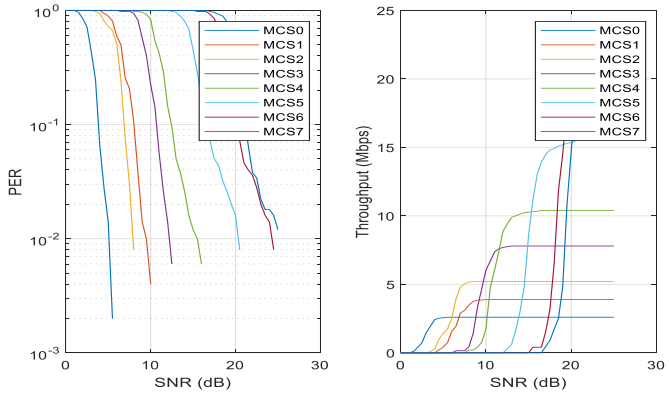

Figure 4.13: Performance of 802.11bd signal model (4 mid-amble period) on the crossing channel

- 802.11bd performance (8 mid-amble period):

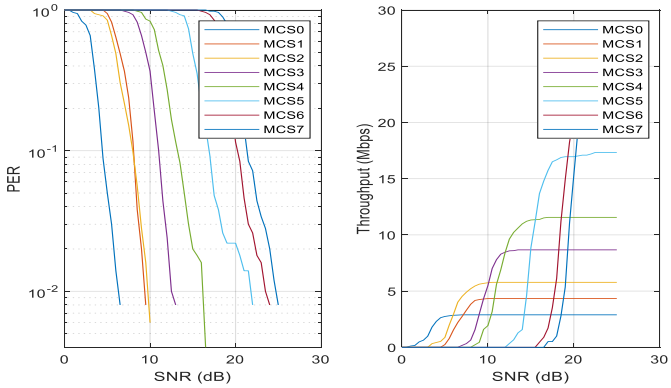

Figure 4.14: Performance of 802.11bd signal model (8 mid-amble period) on the crossing channel

4.3.2 Signal Models Performance Based on the deterministic Channel

The data obtained from Unity program are fed to the V2X simulator as four separate taps per time instant and due to the presence of LOS at our Urban scenario it is expected that the signal models will behave in a similar way as stochastic measurements in the Urban LOS. The modulation and coding schemes used here are shown in table 4.8

MCS value	Coding rate	Modulation type
0	½	BPSK
2	½	QPSK
3	¾	QPSK
4	½	16-QAM
6	2/3	64-QAM

Table 4.5 Modulation and Coding Schemes for Deterministic measurements

The input parameters introduced to the V2X simulator in MATLAB to simulate the channel are:

- The LOS or non-LOS components of each path (h_i), and the LOS initial phase (θ)
- The separate path delays (τ_i) and he input sampling rate ($1/T_s$).
- The Rician factor of each path (K_i), when it's a zero value it represents that this path is Rayleigh fading.
- The Doppler shift of the LOS path ($f_{D_{LOS_0}}$) and the maximum Doppler shift of all paths ($f_{D_{max}}$).
- The Doppler spectrum for each path.

- Performance of 802.11p:

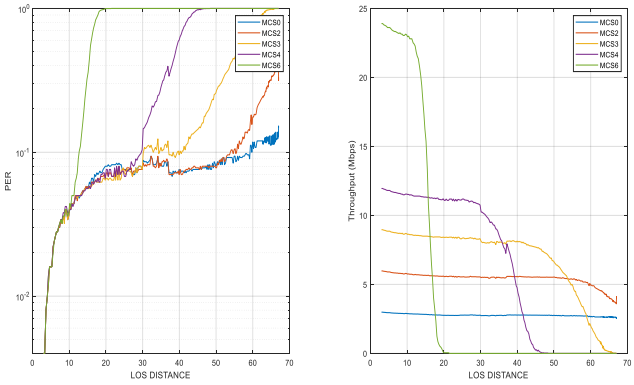

Figure 4.15: Performance of 802.11p signal model on the 3D Unity channel

- Performance of 802.11bd (4 mid-amble period)

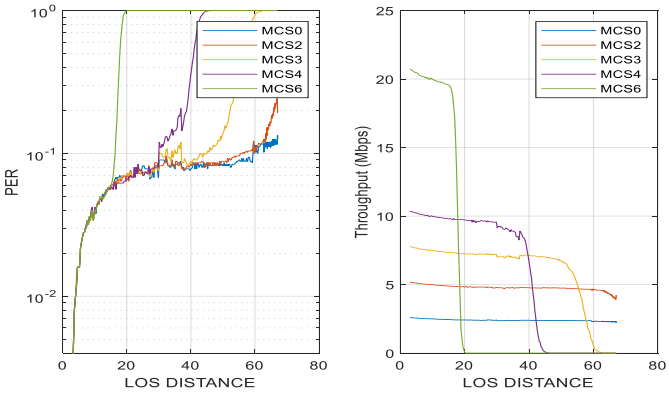

Figure 4.16: Performance of 802.11bd signal model (4 mid-amble period) on the 3D Unity channel

- Performance of 802.11bd (8 mid-amble period):

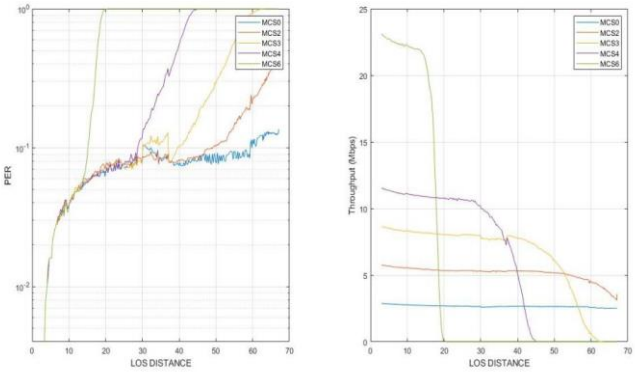

Figure 4.17: Performance of 802.11bd signal model (8 mid-amble period) on the 3D Unity channel

4.4 Results Analysis

4.4.1 Channel Impulse response result Analysis

Figure 4.2 and Figure 4.6 show similar values of the received power at the receiver although two different methods that were used so as to calculate their CIR of the channel designed using Unity program.

4.4.2 Stochastic Channel Result Analysis

As seen from the result Figures (4.6 - 4.14) that are based on the values of the through put and PER on different SNR values and considering the different MCS used:

- In the three different scenarios we can see that the 802.11p signal model have high throughput but a low PER so we need higher SNR value to get a reasonable PER. For the 802.11bd signal model we see a better PER compared to the 802.11p signal model but in the other hand it have lower throughput for each MCS value which is due to addition of the mid-amble pilots that result in a less spectral efficiency.
- The performance of the signal models in the rural LOS and the urban LOS scenarios are quite similar due to the presence of a direct LOS component in both scenarios but due to absence of other vehicles, large fences and buildings in the rural LOS scenario ,it shows a slight better throughput and less PER.
- Due to the absence of a direct LOS component in the street crossing scenario, the performance of the signal models is slight low in terms of throughput and PER compared to the previous scenarios therefore the SNR value should be increased to get similar results as the scenarios where there is a direct LOS

4.4.3 Deterministic channel Result Analysis

As seen from the result Figures (4.17- 4.19) the performance of the signal models in terms of throughput and PER depend on the distance between the TX and RX thus taking the different MCS in consideration:

- when the distance between the TX and RX is reduced the SNR value becomes stronger thus getting improved average PER and throughput.
- The 802.11bd signal model provide better PER but low throughput compared to the 802.11p signal model thus we increase the PER by using eight mid-amble period pilot

,although this will slightly increase the PER but a high throughput is always important.

- The difference in PER between the technologies increases among different values of Doppler shifts with the increase of SNR

4.4.4 Deterministic channel vs Stochastic Channel Result Analysis

- Both Methods resulted in higher performance of the 802.11bd than 802.11p .
- The 802.11bd (4 and 8 mid-ambles) in stochastic measurements showed higher throughput than the deterministic channel. This is due to the many relaxed assumptions considered in the stochastic measurements.
- The results above showed that the performance of the signal models in the deterministic channel experience slight reduction when using higher Modulation and coding scheme which is the opposite in case of the stochastic channel where higher Modulation and coding scheme result in improved throughput and PER values.

CHAPTER 5

Conclusions and Future Work

5.1 Conclusions

The Results discussed in the previous chapter not only provided performance details for the WLAN based V2X system (IEEE 802.11P and 802.11bd),but proved that the vehicular technology is going in the right direction where a recently introduced technology (802.11bd) that is still under development and with uncompleted features is already more reliable , can achieve higher range and throughput compared to the802.11p also it can address all V2X applications in an end-to-end manner with the same technology thus makes it very scalable and future-proof .Moreover, obtaining almost similar results from both the stochastic real time measurements and the deterministic channel model paves the way for more different methods and approaches to through which we can achieve more desirable results and improvements in the V2X System. Some of the extracted conclusions from this thesis include:

- the 802.11bd performance is effected greatly by the Doppler shift that cause channel estimation error where an increase in the Doppler shift deteriorates its performance and as a solution for this midambles are used where ambles are repeated inside data for channel estimation.
- It is important to carefully manage the periodicity of midambles for different vehicle speed since high frequency of midambles Decreases throughput while low frequency of midambles will lead to channel estimation errors.
- Scenarios with dominant LOS show great signal models performance since its affected by the distance between the TX and RX cars.
- Considering the same modulation and code rate, IEEE 802.11bd performs better than 802.11bd in terms of PER and latency .

5.2 Future work

Regarding the future work we can take into consideration the investigation of new scenarios using Unity game program such as increasing the number of cars and their maximum speed as well as changing the starting distances of both the TX and RX cars and adding more non line of sight components. As shown from the results, the performance of the signal models was based on the PER and the throughput, we can include other parameters which are also used for performance analysis such as the Net Data Rates ,Packet Inter-arrival Time and Transmission latency. Simulating the other different type of signal models that are cellular based such as the C-V2X, LTE and 5G can also be considered in the future.

Bibliography

[1] Pin-Han Ho, Hong Wen, Guang Gong, "A Novel Framework for Message Authentication in Vehicular Communication Networks", Department of Electrical Computer Engineering, University of Waterloo, Canada, published by IEEE on 04 March 2010.

[2] L.Nassar, A.Jundi, K.Golestan, Farook Sattar, Fakhri Karray, Mohammed S. Kamel, Slim Boumaiza, "Vehicular Ad-hoc Networks(VANETs): Capabilities, Challenges in Context-Aware processing and Communication Gateway'', Department of Electrical and Computer Engineering, Waterloo, ON N2L 3G1, Canada.

[3] Apoorv saxena, PHY LAYER: IEEE802.11p available at https://apoorvsaxena4.wordpress.com/2015/06/07/phy-layer-ieee-802-11p/., posted on 7 June 2015.

[4] Ali Grami, "Introduction to Digital Communications'', 2016.

[5] Steven W.Smith, Ph.D., "The Scientist and Engineer's guide to Digital Signal Processing'', chapter 6, Second Edition, California Technical Publishing, San Diego, California, 1999.

[6] Sneha H.L, "Basic Signal Operations in DSP: Time shifting, Time Scaling, and Time Reversal'', available at https://www.allaboutcircuits.com/technical-articles/basic-signal-operations-in-dsp-time-shifting-time-scaling-and-time-reversal/, Posted on May 10, 2017.

[7] Gaurang Naik, Biplav Choudhury, Jung-Min Park, "IEEE 802.11bd & 5G NR V2X: Evolution of Radio access technologies for V2X Communications'', Published on May 27, 2019, date of current version June 10, 2019.

[8] Song Gao, Alvin Lim, David Bevly, "An empirical study of DSRC V2V performance in truck platooning scenarios'', Digital Communications and Networks, Volume 2, Issue 4, November 2016, Pages 233-244.

[9] Imad Jawhar, Nader Mohamed, Hafsa Usmani, "An Overview of Inter-Vehicular Communication Systems, Protocols, and Middleware'', Journal of Networks, Vol. 8, NO. 12, December 2013.

[10] Waqar Anwar, Norman Franchi, and Gerhard Fettweis, "Physical layer evaluation of V2X Communications Technologies for 5G NR-V2X, LTE-V2X, IEEE 802.11bd, and IEEE 802.11p'', Vodafone Chair Mobile Communications Systems, Technische Universitat Dresden, Germany, IEEE 90th Vehicular Technology Conference, Honolulu, Hawaii, USA.

[11] Waqar Anwar, Andreas TraBl, Norman Franchi, Gerhard Fettweis, "On the Reliability of NR-V2X and IEEE 802.11bd ", Vodafone Chair Mobile Communications Systems, Technische Universit¨at Dresden, Germany, IEEE 30th Annual International conference Symposium on Personal, Indoor, and Mobile radio communications, Istanbul, Turkey, September 2019.

[12] Andreas Festag, "Standards for vehicular communication from IEEE 802.11p to 5G'', Vodafone Mobile communications, Germany, Published on September 29, 2015.

[13] Molisch, 2011. Wireless Communications, Second Edition, Wiley-IEEE Press.

[14] Carl Gustafson, Kim Mahler, David Bolin, Fredrik Tufesson, "THE COST IRACON Geometry based stochastic Channel model for Vehicle-to-Vehicle Communication in Intersections'', Fraunhofer Heinrich Hertz Institute, Berlin, Germany Mathematical Sciences, Chalmers University of Technology, Gothenburg, Sweden Lund University, Dept. of Electrical and Information Technology, Lund, Sweden.

[15] Loyka, Sergey Kouki, Ammar, "Using Two Ray Multipath Model for Microwave Link Budget Analysis'', IEEE Antennas and Propagation Magazine. 43(5): 31-36, published in October 2001.

[16] Abramowitz, Milton, Stegun, Irene A, "Handbook of mathematical functions with formulas, graphs, mathematical tables'', 1965.

[17] Yochay Lustmann, Danna Porrat, "Indoor channel spectral statistics, K-Factor and Reverberation Distance'', 2010.

[18] MathWorks. [Online] Available at https://se.mathworks.com/help/comm/ref/doppler.html

[19] M. Kahn, "IEEE 802.11 Regulatory SC DSRC Coexistence Tiger Team V2V Radio Channel Models ", December 2014.

[20] MathWorks. [Online] Available at https://se.mathworks.com/help/comm/ug/fading-channels.html.

[21] Pätzold, Matthias, Cheng-Xiang Wang, and Bjorn Olav Hogstand. "Two New Sum-of-Sinusoids-Based Methods for the Efficient Generation of Multiple Uncorrelated Rayleigh Fading Waveforms". IEEE Transactions on Wireless Communications. Vol. 8, Number 6, 2009, pp. 3122–3131.

[22] Oestges, Claude, and Bruno Clerckx. "MIMO Wireless Communications: From Real-World Propagation to Space-Time Code Design''. 1st edition. Boston, MA: Elsevier, 2007.

[23] Kenzi Meyer, Ece Erdogmus, George Morcous, Mary Naughtin, " Use of Ground Penetrating Radar for Accurate Concrete Thickness Measurements'', Architectural Engineering Conference, September 2008.

[24] Payam Vosoughi, Peter Taylor, Halil Ceylan, "Impacts of Internal Curing on the performance of Concrete Materials in the Laboratory and the Fields'', November 2017.

[25] I. Tan, W. Tang, K. Laberteaux and A. Bahai, "Measurement and Analysis of Wireless Channel Impairments in DSRC Vehicular Communications", IEEE International Conference on Communications, Beijing, 2008, pp. 4882-4888.